
Proceedings Paper:

Ibrahim, Y., Mohamad Hardyman, B. and McGregor, J. orcid.org/0000-0001-6813-306X (2021) Assessment of copper-iron catalyst supported on activated carbon for low-temperature nitric oxide reduction by hydrogen. In: IOP Conference Series: Earth and Environmental Science. 1st International Conference on Biomass Utilization and Sustainable Energy 2020 15-16 December 2020, Malaysia, 15-16 Dec 2020, Virtual conference. IOP Publishing .

https://doi.org/10.1088/1755-1315/765/1/012093

IOP Conference Series: Earth and Environmental Science

Assessment of copper-iron catalyst supported on activated carbon for low-temperature nitric oxide reduction by hydrogen

To cite this article: Y Ibrahim *et al* 2021 *IOP Conf. Ser.: Earth Environ. Sci.* **765** 012093

Assessment of copper-iron catalyst supported on activated carbon for low-temperature nitric oxide reduction by hydrogen

Y Ibrahim[1,2,*], B Mohamad Hardyman and McG James[2]

[1] Department of Chemical Engineering and Energy Sustainability, Universiti Malaysia Sarawak, 94300 Kota Samarahan, Sarawak, Malaysia.
[2] Department of Chemical & Biological Engineering, University of Sheffield, Sir Robert Hadfield Building, Mappin Street, Sheffield S1 3JD, United Kingdom.
[3] Department of Cognitive Science, Universiti Malaysia Sarawak, 94300 Kota Samarahan, Sarawak, Malaysia.

*E-mail: yibrahim@unimas.my

Abstract. It is pertinent to assess the performance of a sustainable system that can treat nitrogen oxides (NO_x) emissions from combusting biomass waste. Low-temperature selective catalytic reduction is attractive due to the longer catalyst lifetime and the possibility to use carbon-based catalysts. Hence, this study explores this system with the utilization of: (i) a cost-effective catalyst support, i.e. activated carbon derived from abundant biomass waste; (ii) a renewable reductant, i.e. hydrogen; and (iii) Earth-abundant metal catalysts, i.e. copper and iron. The catalyst was prepared by impregnating metal oxides (Cu and Fe) over palm kernel shell activated carbon (PKS). The catalyst was characterised by hydrogen-temperature programmed reduction (H_2-TPR) and nitric oxide-temperature programmed desorption (NO-TPD). H_2-TPR revealed an increase in the reducibility, attributed to the synergistic effects between Cu and Fe. However, these catalyst sites favour nitrous oxide (N_2O) formation as shown via NO-TPD. Meanwhile, the catalyst activity has also been investigated in a fixed-bed reactor. It showed that the 100% conversion can be achieved at 200°C, but the selectivity towards nitrogen formation is as low as 40%. Therefore, investigating the optimum design of PKSCuFe catalyst is justifiable to improve the performance of low-temperature selective catalytic reduction.

1. Introduction

In developing countries, decomposable organic waste, mainly from agricultural activities, dominates the total solid waste produced (4.5 times more than the generation of municipal solid waste) [1]. Typical final disposal methods are open dumping, landfilling and incineration. The development of methods for the sustainable utilization of solid waste is therefore becoming more prominent [2]. One sustainable alternative in utilizing agro-waste is its conversion to either energy or other useful products, such as composites and activated carbon which have shown successful application in industry. Activated carbon has been utilized widely in wastewater treatment and gas purification processes because it has high adsorption capacity. It is also evident that this material can be potentially utilized in other applications, in particular catalysis. The synthesis and application of carbonaceous catalysts from biomass has recently been reviewed [3]. Additionally, Yang et al. (2011) have reviewed the application of various carbons as catalyst supports for flue gas treatment and concluded that activated carbon can be a potentially cost-effective catalyst support especially for application at low temperature [4].

The conversion of biomass to energy is associated with the emission of greenhouse gases (GHG) including nitrogen oxides (NO_x) and sulphur oxides (SO_x). Pathways for the conversion of biomass into energy include combustion, gasification, fermentation and pyrolysis [5]. In developing countries, even though the energy recovery is usually only 35 % and in some cases 85 %, incineration/combustion is the most common route chosen by developers due to its simplicity, low capital cost (RM 0.55 M/t compared to RM 0.65 M/t for gasification), low operational cost (RM 102/t compared to RM 120/t for gasification) as well as proven technology [6]. Nevertheless, low energy recovery adversely increases the volume of pollutants being released during combustion processes. These include mercury, NO_x gases and volatile organic compounds (VOCs).

NO_x contributes to air pollution and the release of this substance into the atmosphere is strictly regulated by regulations and protocols of the respective countries. Emission of NO_x promotes acid rain and ground-level ozone (smog). Due to the harm that NO_x has brought upon living things, many techniques have been implemented to control the emission of NO_x concentration including gas cleaning technology and selective catalytic reduction (SCR) with the latter being the area of interest lately because of the low capital cost [4], [7]–[10]. However, the operating cost of SCR can be expensive due to the need for ammonia or urea as the reductant. Therefore, other reducing agents have been studied, with hydrogen emerging as a promising alternative which has the potential to be produced sustainably via electrolysis [11], [12].

Many types of catalyst have been tested for NO reduction with hydrogen (H_2-SCR) including Pt [13]–[16] and Pd [17]–[19]. A study using Pt, Pd and Rh supported over aluminium oxide showed high performance above 200 °C with conversion and nitrogen selectivity of at least 95 % and 80 % respectively [20]. The catalysts were also used with other supports including silica [18], zeolite [21], [22], mixed oxides [23], perovskite [24] and cordierite [25], showing favourable adsorption and reduction of nitric oxide. These catalysts and supports however suffer from sustainability issues around resource scarcity due to high demand. The performance of sustainable catalysts, especially those employing Earth-abundant metals and renewable catalyst supports such as activated carbon should therefore be explored.

Copper salt supported on zeolite has been patented to adsorb NO_x at low concentration and shows competitive performance to the noble metals [26]. Furthermore, it has been shown that copper- and iron-exchanged zeolites are reactive at temperatures below 573 K to reduce NO using hydrocarbons, but their performance is still inferior when compared to noble metals catalysts such as platinum [27], [28].

This work aims to tackle the twin challenges of waste utilization and the development of more active and selective H_2-SCR catalysts. Palm kernel shell (PKS), a major residue in oil palm industry, could be an abundant resource for producing carbon catalyst support due to its high carbon content and large surface area [29]. Therefore, it is used in this work as a sustainable carbon source to synthesize the catalyst support, while Earth-abundant metals (Cu and Fe) are employed as the catalytic active agents, both as single component (Cu or Fe only) and as a binary system (Cu and Fe).

2. Methodology

2.1. Catalyst synthesis

PKS activated carbon was supplied by the Universiti Malaysia Sarawak (UNIMAS). The particles were crushed in a ball mill and sieved to obtain uniform size prior to drying in an oven for 72 h at 110 °C. The catalysts were prepared via incipient wetness where the carbon was dipped in a metal salt solution [30] (either copper nitrate trihydrate, iron nitrate nanohydrate or a mixture of copper and iron nitrate, both at 99.999 % trace metals obtained from Sigma-Aldrich, UK). Co-doping was performed by mixing the metal nitrates on a 1:1 mass ratio, keeping the total metal loading as 10 wt.%. Subsequently, the catalysts were dried at 110 °C overnight, washed with deionized water and dried again at 80 °C for 24 h. All catalysts were calcined in an inert nitrogen flow at 200 °C for 2 h.

2.2. Catalyst characterisation

Hydrogen-temperature programmed reduction (H_2-TPR) was performed to investigate the reduction sites and capacity of the catalysts. 0.2 g of the sample was purged under helium flow at 300 °C to remove moisture and volatile components prior to this experiment. The catalyst was reduced under 80 sccm 4 %vol.H_2/He using a programmed-temperature ramp of 2 °C/min from 30 to 400 °C [31]. This experiment was performed in a fixed-bed reactor shown in figure 1. The consumption of hydrogen and formation of water were recorded continuously by mass spectrometry (MS) (Hiden HPR-20, UK), monitoring m/z ratios of 2 and 18 respectively.

To study the nitric oxide adsorption-desorption properties on the catalysts, nitric oxide-temperature programmed desorption (NO-TPD) was carried out in the same reactor by exposing 0.2 g of the sample to 0.3 %vol.NO/He in an 80 sccm flow at room temperature. Subsequently, the flow was switched to pure helium flow and a 2 °C/min temperature ramp was activated. The desorption products were analysed continuously by MS using m/z ratios of 16, 17, 18, 28, 30, 44, 46 for oxygen, ammonia, water, nitrogen, nitric oxide, nitrous oxide and nitrogen dioxide respectively. Some of the ions monitored are common to the fragmentation patterns of more than one species. Therefore, standard gases were analyzed using the MS to obtain a unique fragmentation pattern and relative fragment intensities to indentify the presence of the gas in the sample, and to obtain the intensities contributed by a particular gas [20].

2.3. Catalyst activity experiment

Catalyst testing was conducted in the same reactor as H_2-TPR studies (Section 2.2). The catalyst was reduced at 200 °C under 2 %H_2/He flow of 250 sccm for 120 minutes. The temperature-programmed reaction (TPRxn) was carried out over 1.0 g of catalyst with nitric oxide and hydrogen concentrations of 330 and 8000 ppm respectively in the inlet stream with a temperature ramp rate of 2 °C/min to a final temperature of 450 °C [32].

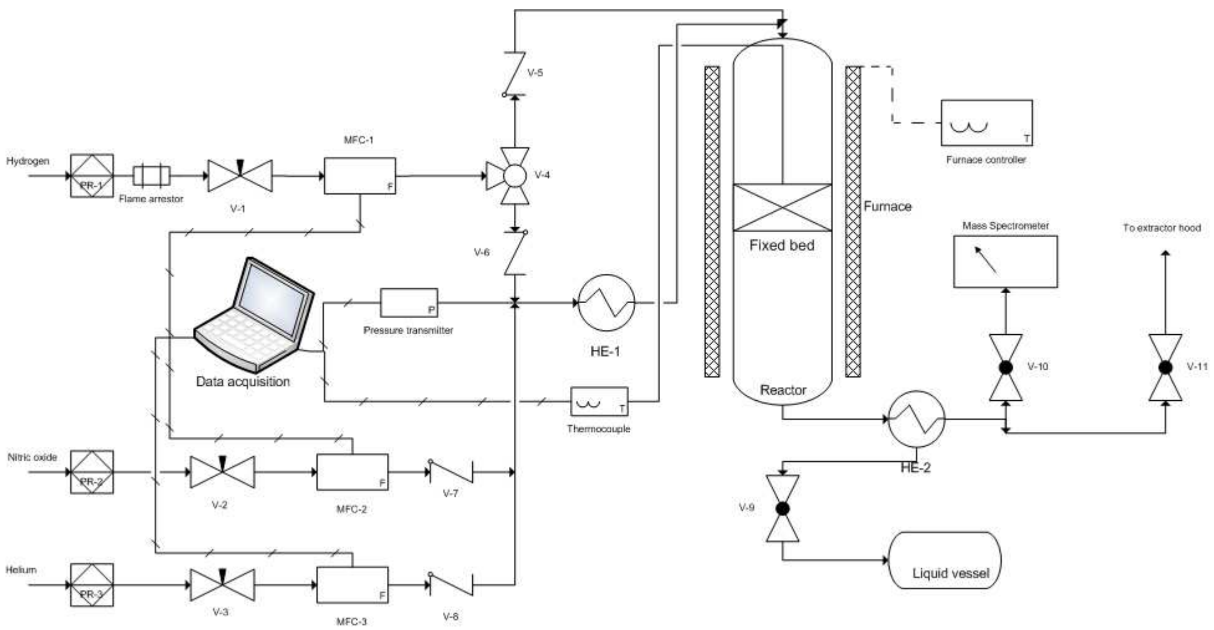

Figure 1. Schematic diagram of the fixed-bed reactor with internal diameter = 7.1 mm. (PR: pressure regulator, V-1 to V-3: isolation valves, V-4: two-way valve, V-5 to V-8: check valves, V-9 to V-11: sampling valves, MFC: mass flow controllers, HE: heat exchangers)

The products were analysed continuously by MS. The calculation of NO conversion (X%) and nitrogen selectivity against N-products (S_{N2}) is based on equations (1) and (2):

$$Conversion\ (X\%) = \frac{Inlet\ NO\text{-}Outlet\ NO}{Inlet\ NO} \times 100\% \tag{1}$$

$$Selectivity\ (S_{N_2}) = \frac{N_2\ formed}{Inlet\ NO\text{-}Outlet\ NO} \times 100\% \tag{2}$$

3. Results and Discussion

3.1. Catalyst characteristics

The effects of introducing iron into copper-activated catalyst have been investigated in respect of the catalyst reducibility and active sites. It is known that the copper reduction temperature (TR) is about 200 °C and the two step reduction ($Cu^{2+} \rightarrow Cu^{+} \rightarrow Cu$) requires higher temperature [33]. As the catalysts in this study have been prepared under mild condition (calcined and reduced at 200 °C), it is not expected that Fe contributes to the reduction of NO as an isolated ion because the reduction temperature of Fe is ~400 °C [34]. Cu_xO_y crystals obtained by heating $Cu(NO_3)_2$ particles give a single TR at 350 °C [35] while on a commercial zeolite-supported catalyst, the TR can be as low as 210 °C [33]. Lamacz et al. (2011) showed that the TR for a copper supported over a ceria-zirconia catalyst can be as low as 150 °C and that the lower TR is correlated with higher metal dispersion [36].

Figure 2 shows two reduction peaks for both catalysts at ~135 and ~309 °C. Therefore, supporting the catalysts on PKS prepared has improved the reducibility of Cu_xO_y. A sharp peak of copper reduction is always attributed to the highly dispersed Cu_xO_y and/or isolated Cu^{2+} ions [35] as can be seen at 135 °C, while reduction at 309 °C can be attributed to the bulk catalyst [37]. Additionally, the higher area under the curve for PKSCuFe shows a greater number of sites have undergone reduction when compared to PKSCu.

Several studies have found that co-catalysts possess lower TR than their counterpart single-component systems. As for example, the lowest TR for Mn/TiO_2, Cu/TiO_2 and $Fe/MnTiO_2$ are 303, 177 and 387 °C, correspondingly. After combining Mn with Cu and Fe, the TR shifted to 129 and 359 °C, respectively for $MnCu/TiO_2$ and $MnFe/TiO_2$ [38]. The deconvolution of the H_2-TPR curve for PKSCuFe (not shown here) identified several peaks between 137 and 312 °C which can be assigned to the Cu-Fe synergistic sites.

The NO-TPD profile for the two catalysts are compared in figure 3. After NO adsorption at room temperature, the catalysts were purged with inert gas. PKSCu (figure 3a) shows desorption of N_2 commencing from 70 °C, and continuing throughout the temperature range. NO exhibits a broad desorption peak between 30 and 180 °C. After the desorption of NO ceases, water is seen to desorb, concurrently with smaller quantities of NH_3. Peaks ascribed to H_2O, NH_3, O_2 and N_2O are all maximized at the same temperature, ~225 °C. No further desorption of water and NH_3 occurs beyond 250 °C but O_2 and N_2O continued to desorb with a second desorption peak centered at ~400 °C. A further distinct N_2O peak was observed at 481 °C, with a shoulder at ~340 °C.

This result suggests that the adsorption of NO on PKSCu at room temperature leads to the formation of nitrogen, nitrous oxide, oxygen, water and ammonia upon desorption at elevated temperature. Additionally, the formation of nitrogen dioxide is also indicated through the simultaneous desorption of NO and O_2 (NO_2 is not stable and rapidly dissociates into NO and O upon desorption) [36]. The decomposition of NO into N_2 is favorable at a wide temperature range which is desirable for an SCR catalyst. In addition, the formation of N_2O, ammonia and water implies some reduction activity on the catalyst sites even in the absence of a reductant, suggesting that functional groups on the surface of the carbon present some catalytic activity.

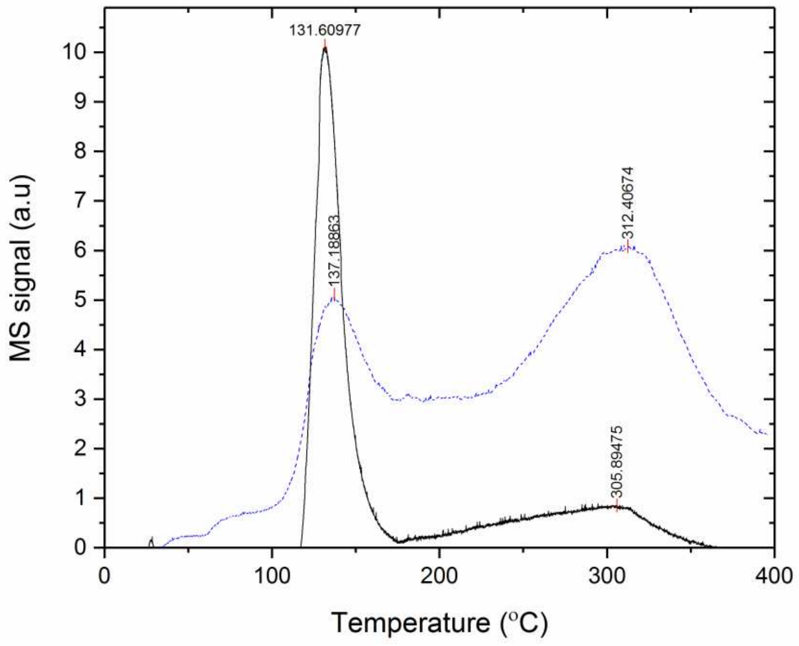

Figure 2. Temperature-programmed reduction at 80 sccm total flow rate with 2 vol.% H_2/He over 0.2 g catalyst and 2 °C/min heating ramp. (black line: —PKSCu, blue dash: – –PKSCuFe)

PKSCuFe contains 50% of the mass of copper as PKSCu; the remainder of the metal content being Fe. However, figure 3b shows that the total amount of NO desorbed in the NO-TPD experiment is similar over both materials at ~419 and 405 ppm for PKSCu and PKSCuFe, respectively. Over PKSCuFe the NO desorption peak is narrower and centered at ~120 °C. Bingnan et al. reported NO desorption at 135 °C for a bare activated carbon prepared from coconut shell, which shifted to 210 °C when the carbon was impregnated with 10 wt.% copper [39]. The low desorption temperature of NO in the present study suggests the presence of physisorbed species, as opposed to the decomposition of nitrates to NO. The latter would be characterized by NO desorption at higher temperatures up to 300 °C [33]. Additionally, no formation of NO_2 is observed over PKSCuFe.

The formation of N_2O is more favorable than N_2 over PKSCuFe. The N_2O peak at ~225 °C is less pronounced over PKSCuFe than for PKSCu, however the peak at ~340 °C is more pronounced. This can be attributed to the synergistic sites of Cu-Fe. Even though the total amount of N_2O evolved is identical in both catalysts, the production of N_2 is reduced by a factor of 2.22 when replacing half of copper, by mass, with iron.

3.2. Nitric oxide adsorption

During the catalyst activity experiment, the catalysts were exposed to NO in order to observe the adsorption behavior at 100 °C. Figure 4 shows the breakthrough curves of the catalyst support (PKS), monometallic copper and iron supported over PKS (PKSCu and PKSFe) as well as the bimetallic catalyst, PKSCuFe. The breakthrough time increases in the order: PKS < PKSFe < PKSCu < PKSCuFe. Adsorption of NO over the bare PKS and iron-impregnated PKS does not form any products (see figures 4a and 4c) showing that physisorption is the only process occurring. When copper is present, in agreement with NO-TPD results, the adsorption is also associated with the production of nitrogen and nitrous oxide (see figures 4b and 4d). The formation of N_2O is observed during the complete adsorption of NO. For PKSCu, the formation of N_2O is replaced by the formation of nitrogen as the partial pressure of NO on the catalyst sites equilibrates with the bulk NO concentration. However, for PKSCuFe, N_2O is continually produced alongside nitrogen because of the affinity of Cu-Fe sites for N_2O production, as confirmed by NO-TPD analysis (Section 3.1).

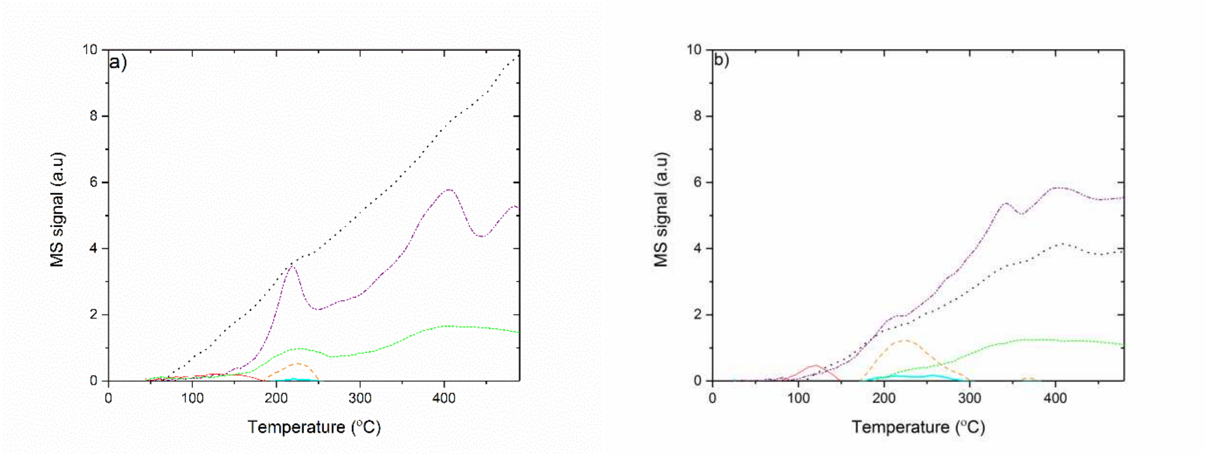

Figure 3. Nitric oxide- temperature-programmed desorption for; a) PKSCu and b) PKSCuFe. 160 sccm total helium flow rate over 0.2 g catalyst and 2 °C/min heating ramp. (—Nitric oxide, – - - –nitrous oxide, ···nitrogen, - - -water, —ammonia, ---oxygen)

As the equilibrium is reached, hydrogen was introduced at excess concentration and the temperature was increased at a constant low rate to investigate the effect of reaction temperature. Figure 5 shows the nitric oxide consumption and the products formed during the reaction. PKS and PKSFe only demonstrated conversion at temperatures in excess of 175 °C while the copper-based catalysts are able to convert NO at temperatures as low as 50 °C. The maximum temperature (T_{max}) and temperature window (temperature from which 50 % conversion is achieved, $T_{50\%}$ to the T_{max}) decreased when iron is incorporated into the catalyst from T_{max} = 125 to 175 °C and $T_{50\%}$ = 115 to 125 °C for PKSCu and PKSCuFe respectively.

From the formation of the by-products, it can be deduced that the following reactions occur on PKSCuFe [23], [24], [40];

$$2NO + 2H_2 \rightarrow N_2 + 2H_2O \tag{3}$$

$$2NO + H_2 \rightarrow N_2O + H_2O \tag{4}$$

$$N_{ads} + N_{ads} \rightarrow N_2 \tag{5}$$

$$N_{ads} + NO_{ads} \rightarrow N_2O \tag{6}$$

$$N_{ads} + 3H_{asd} \rightarrow NH_3 \tag{7}$$

$$NO_{ads} + NH_{x,ads} \rightarrow N_2 + H_xO \tag{8}$$

$$NO_{ads} + NH_{x,ads} \rightarrow N_2O + H_{x,ads} \tag{9}$$

Reactions (3) and (4) are common and well accepted in the study of H_2-SCR where the extent of the reactions determines the selectivity towards N_2 formation. The adsorption of NO and hydrogen on the catalyst surface can initiate the reactions (5) and (6), where N_{ads} indicates the nitrogen atom from NO dissociated during adsorption. In addition, hydrogen can also dissociate upon adsorption as H_{ads} giving rise to the possibility that ammonia is formed by the interaction with N_{ads} as described by reaction (7). Any ammonia produced can also facilitate NO reduction with hydrogen as shown in equations (8) and (9) resulting in competing reduction pathways [40]. Additionally, significant production of N_2O occurs on PKSCuFe but the formation of ammonia is suppressed, occurring at a higher temperature as compared to on PKSCu.

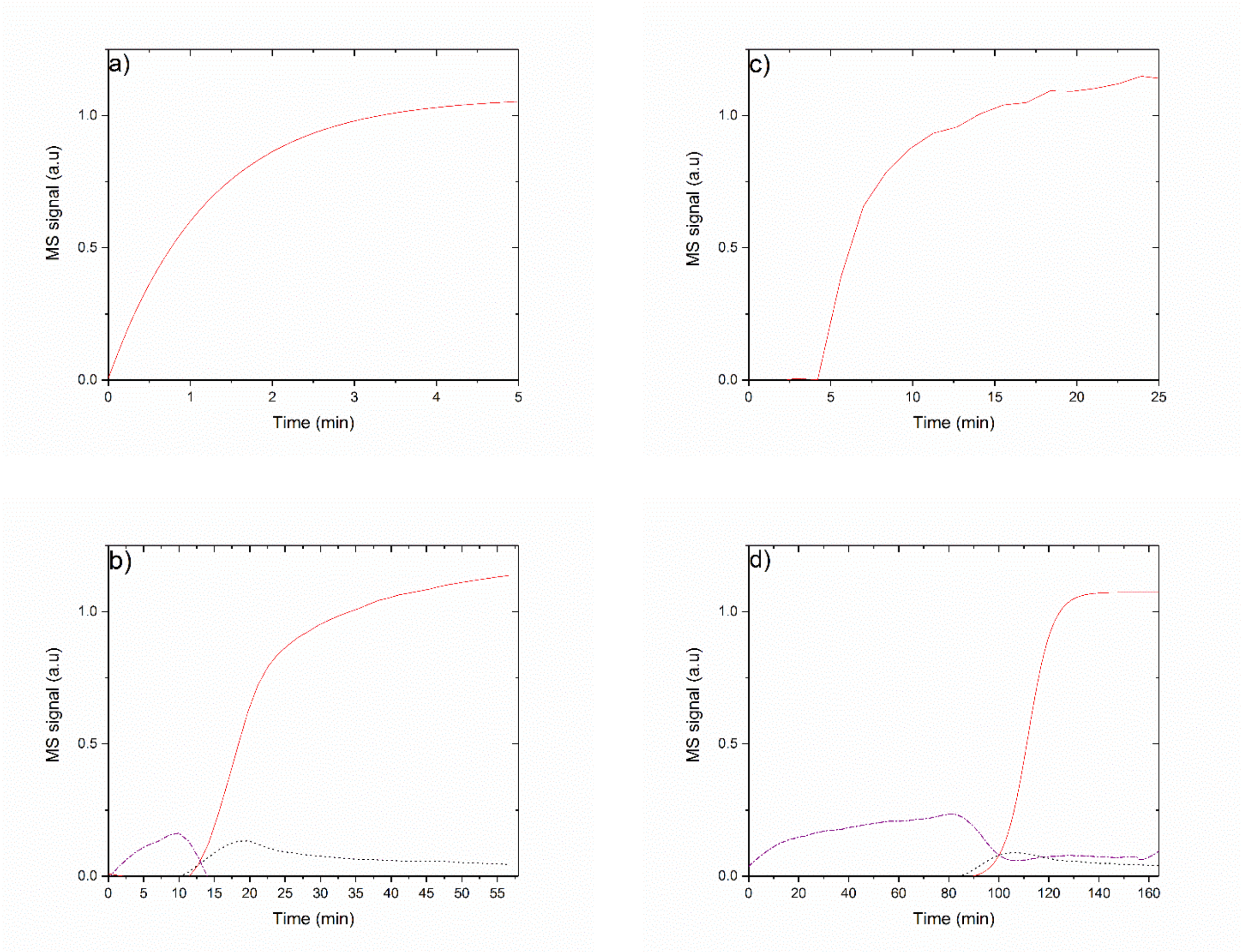

Figure 4. Adsorption profile for; a) PKS, b) PKSCu, c) PKSFe, and d) PKSCuFe. 250 sccm total flow of 330 ppm NO + 8000 ppm H_2 at atmospheric pressure and 100 °C over 1.0 g catalyst. (—Nitric oxide, – - - –nitrous oxide, ···nitrogen)

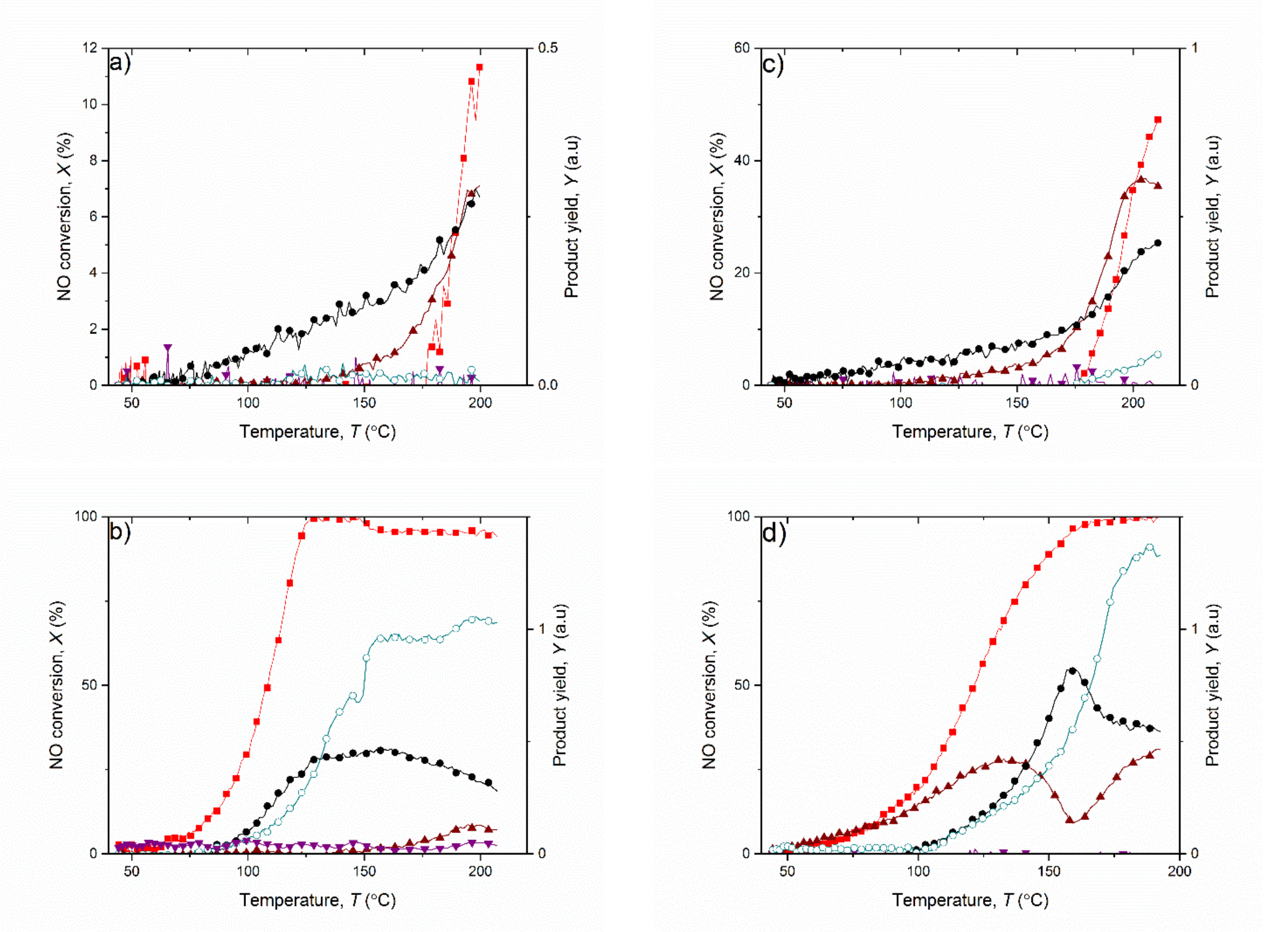

Figure 5. Temperature-programmed reaction profiles for; a) PKS, b) PKSCu, c) PKSFe, and d) PKSCuFe. 250 sccm total flow of 330 ppm NO + 8000 ppm H_2 at atmospheric pressure and increasing temperature from 40 to 200 °C by 2 °C/min over 1.0 g catalyst. (■Converted nitric oxide, ▲Nitrous oxide, ●Nitrogen, ○Ammonia, ▼Nitrogen dioxide)

3.3. Nitric oxide reduction

Commercial copper catalyst (9.2 %Cu-mordenite) and ferric catalyst (4.7 % Fe_2O_3) have shown 95 % NO_x conversion by NH_3 in the range of 224 – 440 °C and 310 – 560 °C, respectively [41]. As the temperature used in this work is lower than in those studies, the conversion is expected to be lower. Figure 6 depicts the relationship between the catalyst performance in terms of NO conversion and N2 selectivity for PKSCu and PKSCuFe. For PKSCu, the conversion reaches its maximum plateau beyond 150 °C at 96 % while selectivity decreases with temperature reaching 38 % at 200 °C. Considering PKSCuFe, constant conversion is also achieved at 150 °C but the selectivity has a maxima at 160 °C with 60 % of NO converted to N_2. The low selectivity as compared to the manganese-based TiO_2-supported catalysts is due to the formation of ammonia and nitrous oxide [38].

As hydrogen is in excess, the reaction is presumed to be first order, equation (10), with regards to NO and the Arrhenius behavior, equation (11), is assumed:

$$r = k[NO] \tag{10}$$

$$k = Ae^{-E_a/RT} \tag{11}$$

where r is the rate of reaction (mol/g.s), k is the reaction constant (/s), [NO] is the NO concentration (mol), A is the pre-exponential constant (/s), E_a is the apparent activation energy (kJ/mol), R is the universal gas constant (8.314 X 10^{-3} kJ/mol.K) and T is the reaction temperature (K). Five temperatures were selected from 80 to 200 °C to study the effect of the temperature on the reaction parameters. Figure 7 shows the Arrhenius plot for PKSCu and PKSCuFe where it can be seen that E_a decreases by almost 30 % from 96.86 to 69.50 kJ/mol when using PKSCu and PKSCuFe respectively. Both values are relatively high when compared to the reported values for NH_3-SCR with zeolitic materials (including some with copper loading) which range from 24 to 89 kJ/mol [42].

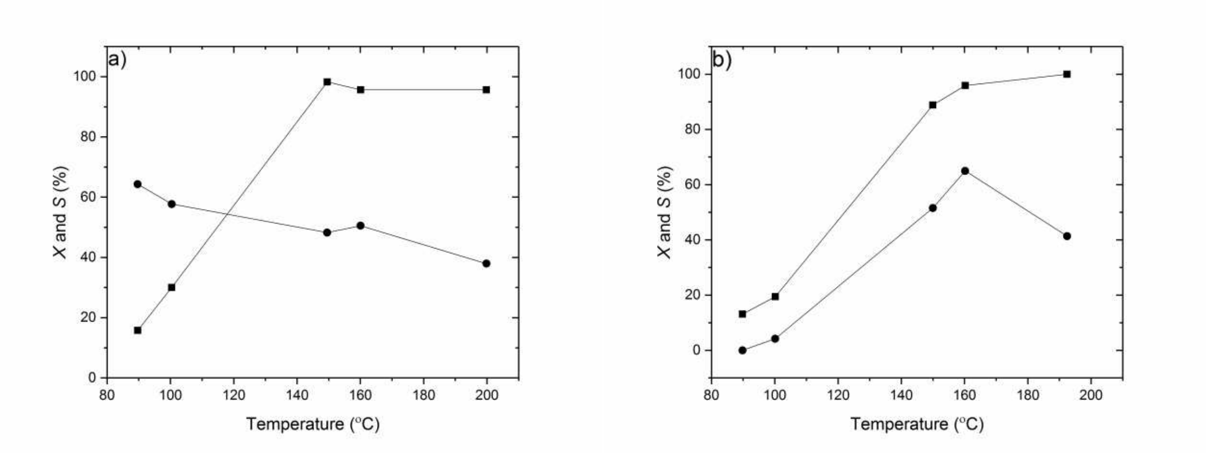

Figure 6. Conversion (■X) and selectivity (●S) profiles for; a) PKSCu and b) PKSCuFe. 250 sccm total flow of 330 ppm NO + 8000 ppm H_2 at atmospheric pressure and temperature from 90 to 200 °C by 2 °C/min over 1.0 g catalyst.

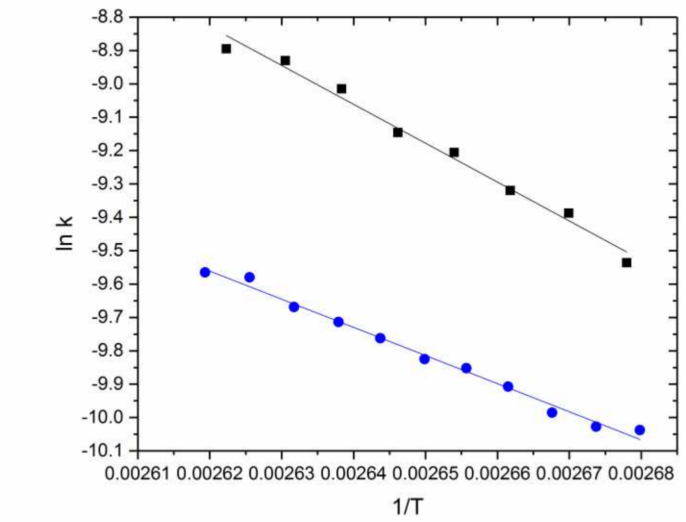

Figure 7. Arrhenius plot. (■PKSCu, ●PKSCuFe)

4. Conclusion

Copper-iron catalyst (PKSCuFe) was prepared under mild conditions using active carbon prepared from palm kernel shell (PKS) as the support *via* incipient wetness. In order to investigate the role of Cu-Fe in a hydrogen-selective catalytic reduction (H_2-SCR), monometallic catalysts of copper (PKSCu) and iron (PKSFe) were also synthesized using the same carbon support. Temperature-programmed reduction of PKSCu and PKSCuFe shows two main peaks at ~135 and ~309 °C that are attributed to highly dispersed Cu_xO_y and/or isolated Cu^{2+} ions and to the bulk catalyst respectively. In addition, PKSCuFe possess synergistic Cu-Fe sites that increases the reducibility of the copper-carbon system. Nitric oxide-temperature-programmed desorption demonstrates that NO is both physisorbed and chemisorbed, with the latter leading to the formation of nitrogen, nitrous oxide, oxygen, water and ammonia. Additionally, PKSCuFe shows higher basicity strength compared to PKSCu, resulting in the formation of N_2O. This phenomena has been corroborated by adsorption studies conducted at 100 °C where N_2O is continually evolved during the adsorption over PKSCuFe. PKSCuFe has the longest NO breakthrough time among the other materials used (PKS, PKSFe and PKSCu). As hydrogen was added into the system, NO reduction occurs commencing at temperatures as low as 50 °C over PKSCu and PKSCuFe. The maximum temperature and temperature window decreased when comparing PKSCuFe with PKSCu. Several possible reactions from the literature have been proposed to take place during the reaction which alter the selectivity towards nitrogen formation. Arrhenius plots for PKSCu and PKSCuFe show that PKSCuFe presents a lower activation energy. These findings motivate the development of a sustainable catalyst for H_2-SCR as an attractive alternative in mitigating nitrogen oxide emissions.

References

[1] Kaza S, Yao L, Bhada-Tata P, Woerden F Van. 2018 *What a Waste 2.0: A Global Snapshot of Solid Waste Management to 2050.*

[2] Dhokhikah Y, Trihadiningrum Y 2012 *J Appl Environ Biol Sci.* **2**(7) 329–35.

[3] Davies G, El Sheikh A, Collett C, Yakub I, McGregor J 2020 Catalytic carbon materials from biomass In: Sadjadi S, editor. *Emerging Carbon Materials for Catalysis* Amsterdam: Elsevier 161–95.

[4] Yang Y, Chiang K, Burke N 2011 *Catal Today* **178**(1) 197–205.

[5] Mohammed M A A, Salmiaton A, Wan Azlina W A K G, Mohammad Amran M S, Fakhru'L-Razi A, Taufiq-Yap Y H 2011 *Renew Sustain Energy Rev.* **15**(2) 1258–70.

[6] Peterson D, Haase S 2009 Market assessment of biomass gasification and combustion technology for small- and medium-scale applications market assessment of biomass gasification and combustion technology for small- and medium-scale applications Technical Report NREL/TP-7A2-46190.

[7] Shang X, Hu G, He C, Zhao J, Zhang F, Xu Y 2012 *J Ind Eng Chem.* **18**(1) 513–9.

[8] Kubinski D J, Visser J H 2008 *Sensors Actuators, B Chem.* **130**(1) 425–9.

[9] Wang L, Liu Z, Li P, Yu J, Rodrigues A E 2012 *Chem Eng J.* **197** 151–61.

[10] Benson SA, Laumb J D, Crocker CR, Pavlish J H 2005 *Fuel Process Technol.* **86**(5) 577–613.

[11] Hamada H, Haneda M 2012 *Appl Catal A Gen.* **421–422** 1–13.

[12] Savva P G, Costa C N 2011 *Catal Rev.* **53**(2) 91–151.

[13] Lindholm A, Currier NW, Fridell E, Yezerets A, Olsson L 2007 *Appl Catal B Environ.* **75** 78–87.

[14] Zhang X, Wang X, Zhao X, Xu Y, Liu Y, Yu Q 2015 *Chem Eng J.* **260** 419–26.

[15] Yuan L, Zheng X, Duan K, Hu H, Wang J, Woo SI 2013 *Front Environ Sci Eng.* **7**(3) 457–63.

[16] Tu B, Shi N, Sun W, Cao L, Yang J 2017 *Environ Sci Pollut Res.* **24**(1) 676–84.

[17] Qi G, Yang R, Rinaldi F 2006 *J Catal.* **237**(2) 381–92.

[18] Yin C, Wang L, Rivillon S, Shih A J, Yang R T 2015 *Catal Letters* **145** 1491–9.

[19] Caravaggio G, Nossova L, Burich R 2016 *Emiss Control Sci Technol.* 2016 **2**(1) 10–9.

[20] Mihet M, Lazar M D, Almasan V, Mirel V 2012 H_2-SCR at low temperatures on noble metal supported catalysts In: *AIP Conference Proceedings* 73–6.

[21] Yang S, Wang X, Chu W, Song Z, Zhao S 2011 *Appl Catal B Environ.* **107**(3–4) 380–5.

[22] Yu Q, Richter M, Kong F, Li L, Wu G, Guan N 2010 *Catal Today* **158**(3–4) 452–8.
[23] Costa C 2002 *J Catal*. **209**(2) 456–71.
[24] Chiarello G L, Ferri D, Grunwaldt J D, Forni L, Baiker A 2007 *J Catal*. **252**(2) 137–47.
[25] Lindholm A, Currier N W, Dawody J, Hidayat A, Li J, Yezerets A 2009 *Appl Catal B Environ*. **88**(1–2) 240–8.
[26] Shigenori O, Nara Masayoshi I 1991 Methods of Removing NO_x by Absorption, NO_x Adsorbent and Apparatus for Purifying NO_x Containing Gas OTW 1–6.
[27] Shin HK, Hirabayashi H, Yahiro H, Watanabe M, Iwamoto M 1995 *Catal Today* **26**(1) 13–21.
[28] Li J, Chang H, Ma L, Hao J, Yang R T 2011 *Catal Today* **175**(1) 147–56.
[29] Nizamuddin S, Shrestha S, Athar S, Ali B S 2016 *Rev Chem Eng* **32**(5) 1–17.
[30] Haber J, Block J H & Delmon B 1995 *Pure Appl Chem* **67**(8–9) 1257–1306.
[31] Zhang X, Wang X, Zhao, X, Xu Y, Gao H, Zhang F 2014 *Chem Eng J* **252** 288–297.
[32] Tan M, Yakub I, Yun Hin T-Y 2020 *J Appl Sci Proc Eng* **7**(1) 479–488.
[33] Ma L, Cheng Y, Cavataio G, McCabe R W, Fu L, Li J 2013 *Chem Eng J*. **225** 323–30.
[34] Sreekanth P M, Smirniotis P G 2008 *Catal Letters* **122**(1–2) 37–42.
[35] Bhaduri B, Verma N 2015 *J Colloid Interface Sci*. **457** 62–71.
[36] Li Y, Armor J N 1991 *Appl Catal*. **76** L1–8.
[37] Yuan D, Li X, Zhao Q, Zhao J, Tadé M, Liu S 2014 *J Catal*. **309** 268–79.
[38] Thirupathi B, Smirniotis P G 2011 *Appl Catal B Environ*. **110** 195–206.
[39] Bingnan F, Guanzhong L, Yanqin W, Yun G, Yanglong G 2011 *Chinese J Catal*. **32**(5) 853–61.
[40] Park S M, Kim M Y, Kim E S, Han H S, Seo G 2011 *Appl Catal A Gen*. **395**(1–2) 120–8.
[41] Kułażyński M. 2011 Selective catalytic reduction NO by ammonia over ceramic and active carbon based catalysts. In: Ahsan A, editor. *Heat Analysis and Thermodynamics Effects* InTech.
[42] Kwak J H, Tran D, Szanyi J, Peden C H F, Lee J H 2012 *Catal Letters*. **142**(3) 295–301.

Acknowledgements

The authors would like to thank the Universiti Malaysia Sarawak for the Cross Disciplinary Research grant F02/CDRG/1843/2019.